The 6th International Supercritical CO_2 Power Cycles Symposium
March 27 - 29, 2018, Pittsburgh, Pennsylvania

Simulation of SCO_2 Oxy-Combustion Using Reduced Chemical Kinetic Mechanism: Effects of Reduced Mechanism and Sensitivity to Mechanism Parameters

Zefang Liu
Graduate Student
Georgia Institute of Technology
Atlanta, GA

Xiang Gao
Ph.D.
Georgia Institute of Technology
Atlanta, GA

Miad Karimi
Graduate Student
Georgia Institute of Technology
Atlanta, GA, USA

Bradley Ochs
Research Engineer II
Georgia Institute of Technology
Atlanta, GA

Vishal Acharya
Research Engineer II
Georgia Institute of Technology
Atlanta, GA

Wenting Sun
Assistant Professor
Georgia Institute of Technology
Atlanta, GA

Jacob Delimont
Research Engineer
Southwest Research Institute
San Antonio, TX, GA

Nathan Andrews
Research Engineer
Southwest Research Institute
San Antonio, TX, GA

ABSTRACT

Current research on supercritical carbon dioxide (SCO_2) oxy-combustion is lacking studies on the performance of kinetic models. An optimized 13 species kinetic model is proposed in the present work for $CH_4/O_2/CO_2$ oxy-combustion. This 13 species kinetic model is developed based on the detailed USC Mech II mechanism with the Global Pathway Selection (GPS) algorithm, and then optimized with a genetic algorithm covering conditions of pressure from 150 atm to 300 atm, temperature from 900 K to 1800 K and equivalence ratio from 0.7 to 1.3. The autoignition of 13 species kinetic model presents less than 12% error relative to that of the USC Mech II. The performance of the proposed kinetic model is evaluated using a generic jet in crossflow combustor. Simulations at identical conditions are conducted in ANSYS Fluent for the 13 species model, a global 5 species model from Fluent and a 24 species model simplified from GRI Mech 3.0 with GPS. Results were then compared to evaluate the sensitivity of these three kinetic models to the CFD simulations. The results show a slower temperature raising, a longer autoignition delay and a smaller laminar flame speed using the 13 species kinetic model. It is indicating the importance of choice on kinetic models in numerical simulation.

NOMENCLATURE

A	pre-exponential factor
D	diameter
E	energy
H	hydrogen
k	rate constant
L	length
P	pressure
T	Temperature

Greek

β	temperature dependence
τ	time of autoignition delay
ϕ	equivalent ratio, angle

Subscripts

0	initial
A	activation
ign	ignition

INTRODUCTION

Directly fired supercritical carbon dioxide (SCO_2) oxy-combustion power cycle has the potential to increase the efficiency and capture up to 99% of carbon produced in the combustion process [1]. This power cycle works at extreme pressure conditions of around 200 bar to 300 bar. To facilitate the development of combustors for directly fired SCO_2 power cycle, a reliable kinetic model is needed. However, developing an appropriate kinetic model is impeded by significant challenges of the extreme operating conditions at high pressure (over 100 bar and up to 300 bar), high inlet temperature (over 900K) and rich CO_2 dilution (up to 96%). In addition, there is no relevant experimental kinetic data for kinetic model validation above the critical pressure of CO_2 for mixtures with high CO_2 concentration. This motivates the need to perform numerical studies to evaluate the sensitivity of the simulation to different kinetic models and provide guidance for kinetic model selection. Past study by Iwai et al. [2] numerically investigated preliminary design of a combustor for SCO_2 power cycle. Part of the reacting flow analysis was conducted by using a NUIG kinetic model [3] and part of the reacting flow analysis was conducted using GRI 3.0 [6]. similar fluid properties and temperature were obtained. Then GRI 3.0 was used because of its convenience [2]. Nevertheless, numerical simulations with detailed kinetic models require very large computational resource owing to the large number of species contained in the models. For example, the USC Mech II [4] contains 111 species and thus, a numerical simulation using this mechanism is prohibitively expensive.

In this paper, preliminary evaluation of kinetic models using newly obtained autoignition delay data for $CH_4/O_2/CO_2$ mixture at 105 bar was performed. Then a reduced and optimized kinetic model is presented for methane (CH_4) SCO_2 oxy-combustion using USC Mech II [4]. ANSYS Fluent [5] simulations of a generic jet in crossflow typed combustor are conducted using the developed reduced and optimized kinetic model, a global kinetic model containing only 5 species, and a 24 species kinetic model simplified from GRI Mech 3.0 with GPS, respectively. These simulations using three different kinetic models are compared and the suggestion for kinetic model selection is given.

KINETIC MODEL REDUCTION AND OPTIMIZATION

For the development of the reduced and optimized kinetic model at the relevant SCO_2 operating conditions, a candidate kinetic model needs to be selected. Figure 1 shows autoignition delay measurement of $CH_4/O_2/CO_2$ (mole fraction 5/10/85) at 105 atm from the Georgia Tech high pressure shock tube compared with the numerical simulation using different kinetic models (USC Mech II [4], GRI Mech 3.0 [6], HP-Mech [8][9], Aramco 2.0 [10]). The shock tube used in this study is fabricated out of stainless steel 316 with 15.24 cm inner diameter and wall thickness of 5.08 cm. The total length of the shock tube is 20 m consisting of 10 m long driver section and 10 m long driven section. The temperature uncertainty owing to the uncertainty in the shock velocity is found to be approximately ±10 K. The sidewall pressure histories are recorded by a Kistler 6045A PiezoStar dynamic pressure sensor located at 1.3 cm away from the end wall. OH* emission from the sidewall was used to monitor the ignition.

Although autoignition delay data at SCO_2 condition are very limited, Figure 1 shows the first autoignition delay measurement at SCO_2 condition in record. The plot also shows the autoignition calculation using different kinetic models, including USC Mech II [4], GRI Mech 3.0 [6], HP-Mech [8][9], Aramco 2.0 [10]. As shown in Fig. 1, simulation results from Aramco 2.0 [10], USC Mech II [4] and HP-Mech [8][9] are close to each other with a maximum deviation of 12%. GRI 3.0 [6] predicts a significantly shorter autoignition delay, having approximately a factor of 3 difference. Experimental measurements fall between the prediction of USC Mech II [4] and GRI 3.0 [6] and appear to have better agreement with

predictions from USC Mech II [4]. The experimental results deviate approximately 40% for USC Mech II and 100% for GRI 3.0 [6]. Since USC Mech II has the best agreement with the experimental result. This observation is consistent with results in Ref. [1]. Therefore, USC Mech II was selected as the candidate kinetic model for the further reduction and optimization.

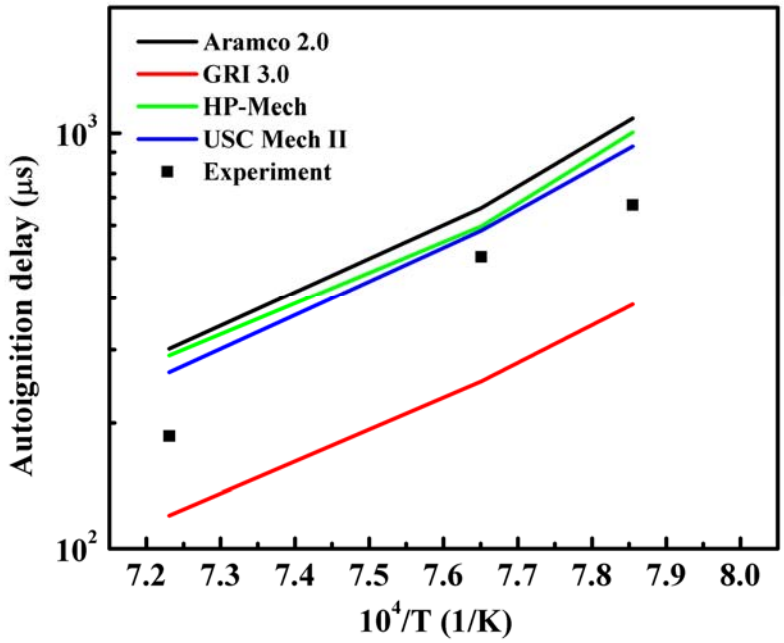

Figure 1. Comparison of measured autoignition delays of $CH_4/O_2/CO_2$ mixture (5:10:85) and simulation using different kinetic models at 105 atm

The USC Mech II [4] contains 111 species and 784 reactions, resulting in expensive CPU time, thus necessitating the need for a reduced kinetic model. This is obtained by Global Pathway Selection [11] reduction algorithm and an in-house developed genetic algorithm as discussed below. This reduced and optimized kinetic model is validated using a zero-dimensional reactor and then employed to simulate a generic jet in the crossflow combustor.

In previous work, Coogan et al. [1] proposed a 27-species reduced kinetic model based on the Global Pathway Selection method (GPS) [11]. This kinetic model still requires significant resource and time to compute in Fluent for the combustor simulation. In the present work, the 27 species model is further reduced to a 13 species kinetic model, including CH_4, CH_3, CH_2O, HCO, CO, H, O, O_2, OH, H_2O, H_2O_2, HO_2, and CO_2, and 46 reactions. However, this further reduction increases errors (results before optimization are shown in Figure 2, which give more than 100% error, especially for the higher temperature), so the reaction rate parameters need to be optimized.

For this purpose, a genetic algorithm [12] is integrated in Cantera [13]. It is an analogue of natural selection processes. At the beginning, a population of candidate kinetic models are initiated with random perturbations of the reaction rate parameters. Then, the fitness of each kinetic model is measured by the accuracy. The kinetic models with greater fitness have the higher probability to be selected to generate the next generation of candidate kinetic models. This is done by merging the “parent” kinetic models. This process is repeated until the desired accuracy is achieved or the maximum number of generations is reached. In the present work, the accuracy is defined as the negative relative error of the simulated autoignition delays compared to the simulated autoignition delays obtained by the detailed mechanism, i.e. USC Mech II. The conditions cover pressure ranging from 150 atm to 300 atm, initial temperature ranging from 900K to 1800K, and equivalence ratio from 0.7 to 1.3. With such optimization technique, the error of the 13 species mechanism is reduced to less than 12% after 7-round optimization, as shown in Figure 3.

In Figure 2 and Figure 3, “detailed” means results from detailed USC Mech II, “original” means results from reduced 13 species model before optimization, and “optimized” means results from optimized 13 species model.

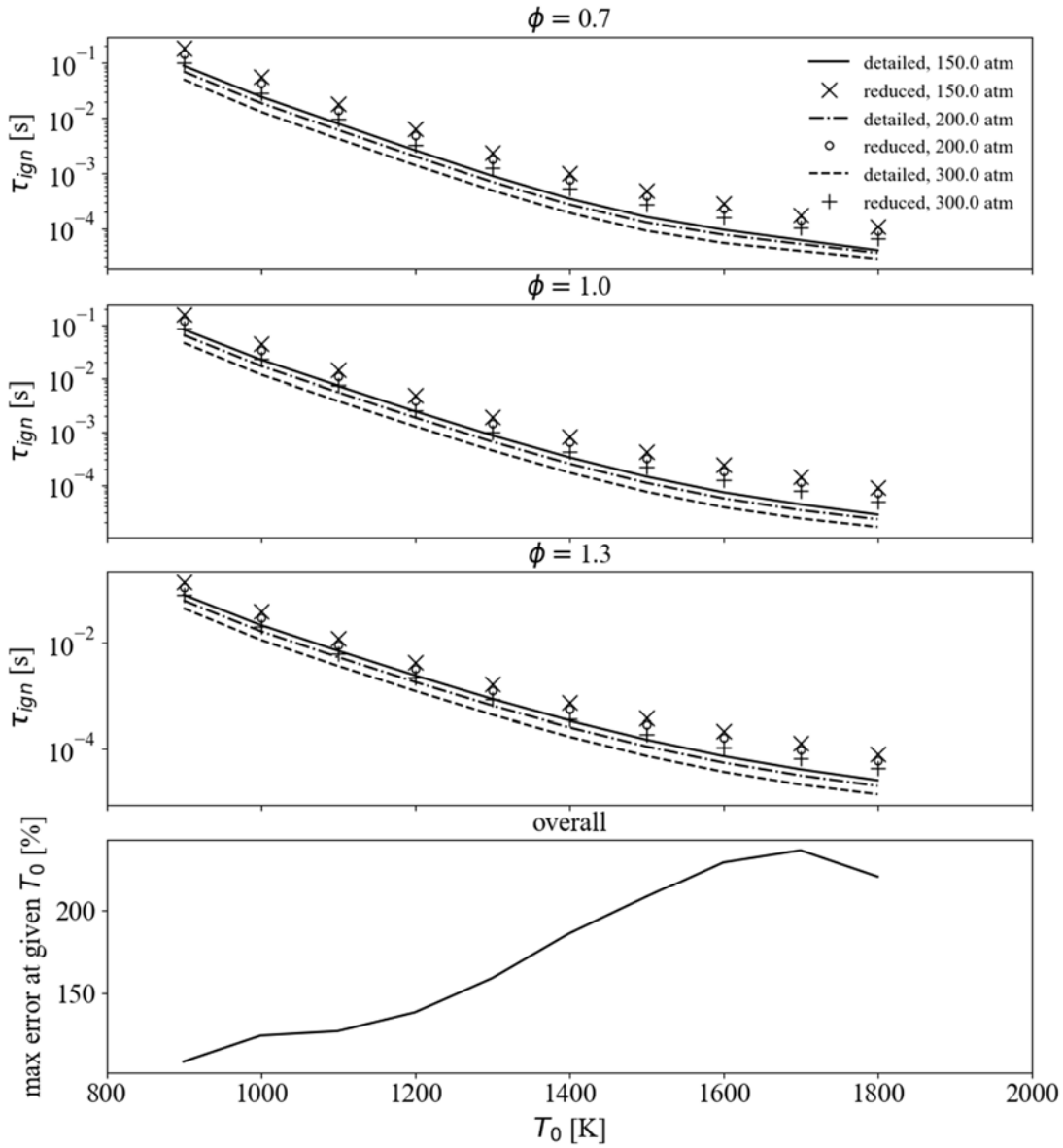

Figure 2. Comparison of autoignition delays at different conditions between the detailed kinetic model and the reduced kinetic model before optimization and their associated errors

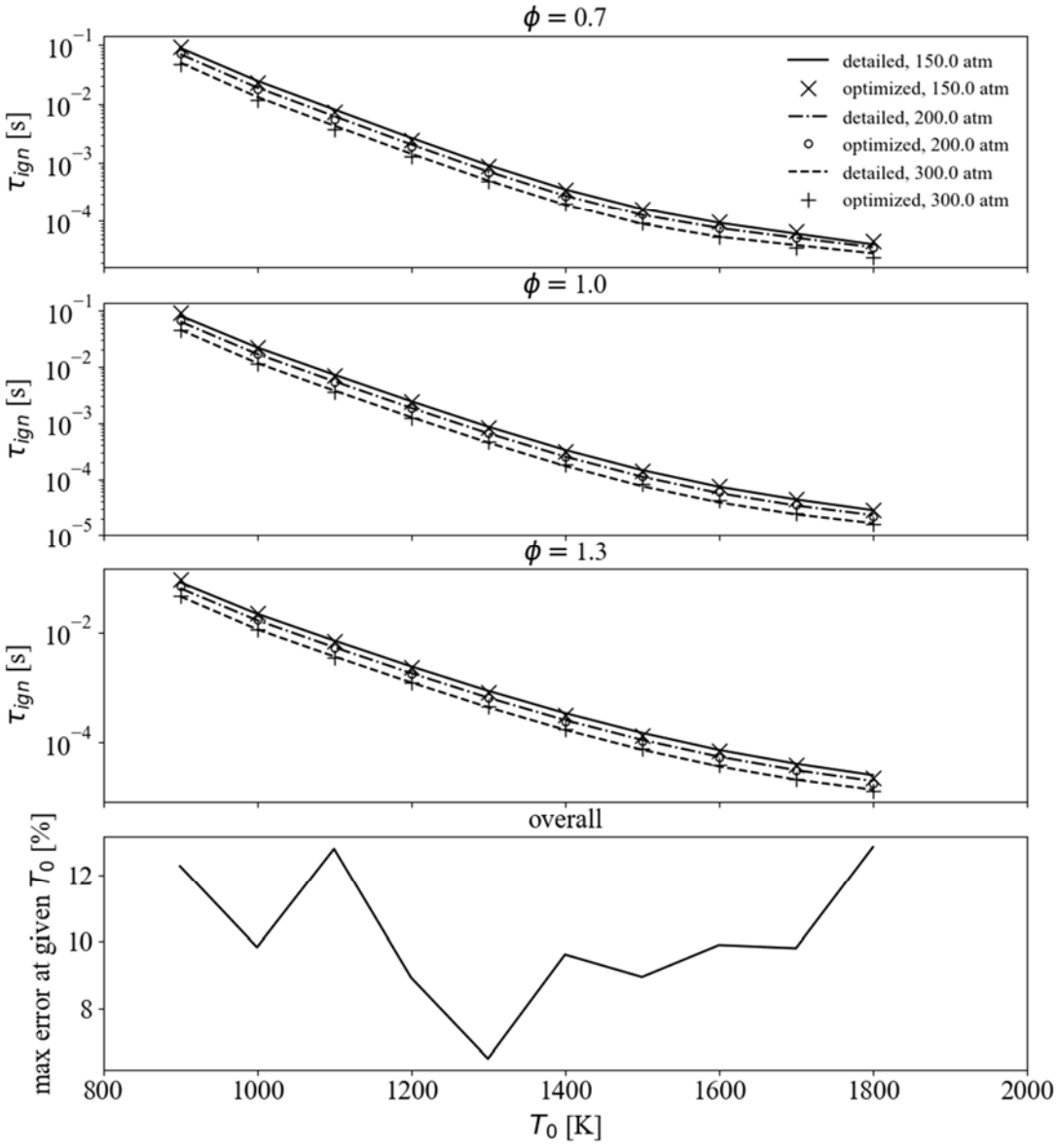

Figure 3. Comparison of autoignition delays at different conditions between the detailed kinetic model and the reduced kinetic model after optimization and their associated errors

COMPARISON OF 5-SPECIES, 13-SPECIES, AND 24 SPECIES KINTEIC MODELS

In this section, the ANSYS Fluent [5] simulation of a generic combustor was conducted using a global 5 species kinetic model in-built in Fluent, the optimized 13 species kinetic model and a 24 species kinetic model with 130 reactions simplified from GRI Mech 3.0 with GPS [11]. The 5 species global kinetic model consists of 3 reactions and has been presented in Table 1.

Table 1. 5 species 3 reactions model from Fluent

Reaction No.	1	2	3
Reaction	$CH_4 + 1.5O_2 \rightarrow CO + 2H_2O$	$CO + 0.5O_2 \rightarrow CO_2$	$CO_2 \rightarrow CO + 0.5O_2$
Reactions rate	$\frac{d[CH_4]}{dt} = -k_{f,1}[CH_4]^{0.7}[O_2]^{0.8}$	$\frac{d[CO]}{dt} = -k_{f,2}[CO]^{1}[O_2]^{0.25}$	$\frac{d[CO_2]}{dt} = -k_{f,3}[CO_2]^{1}$
Arrhenius equation	$k_{f,1} = A_1 T^{\beta_1} e^{-\frac{E_1}{RT}}$	$k_{f,2} = A_2 T^{\beta_2} e^{-\frac{E_2}{RT}}$	$k_{f,3} = A_3 T^{\beta_3} e^{-\frac{E_3}{RT}}$
$\frac{A}{\left(\frac{kmol}{m^3}\right)^{1-\alpha-\beta}\left(\frac{1}{s}\right)}$	5.012×10^{11}	2.239×10^{12}	5×10^{8}
β/K	0	0	0
$E_A/J \cdot kmol^{-1}$	2×10^{8}	1.7×10^{8}	1.7×10^{8}

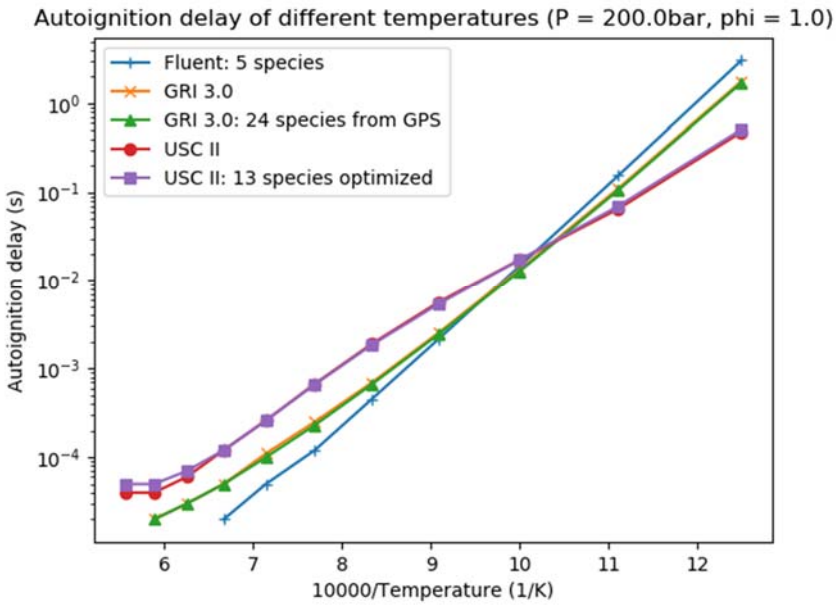

Figure 4. Autoignition delay of different temperatures for different kinetic models with 200 bar and stoichiometric equivalence ratio (94.13% CO_2 dilute)

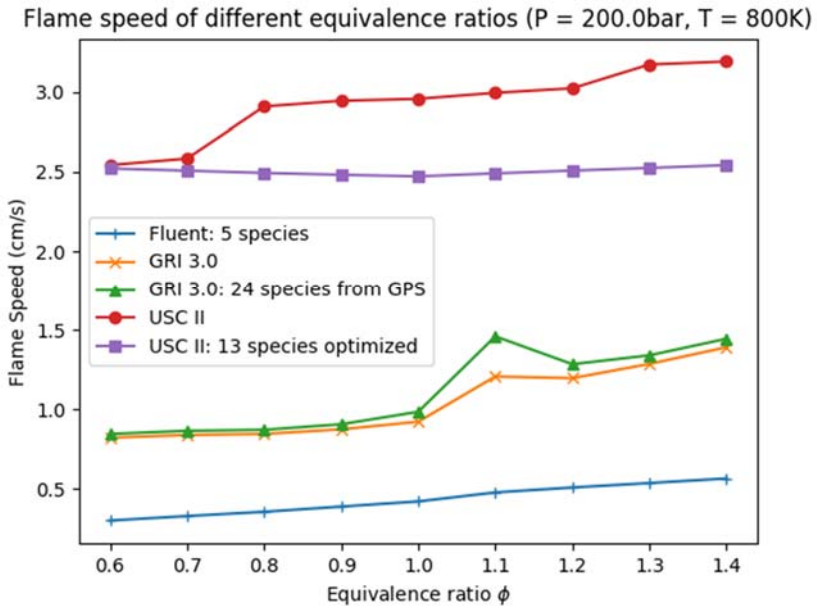

Figure 5 **Laminar flame speed (unit: cm/s) of different equivalence ratios for different kinetic models with 200 bar and initial temperature 800K**

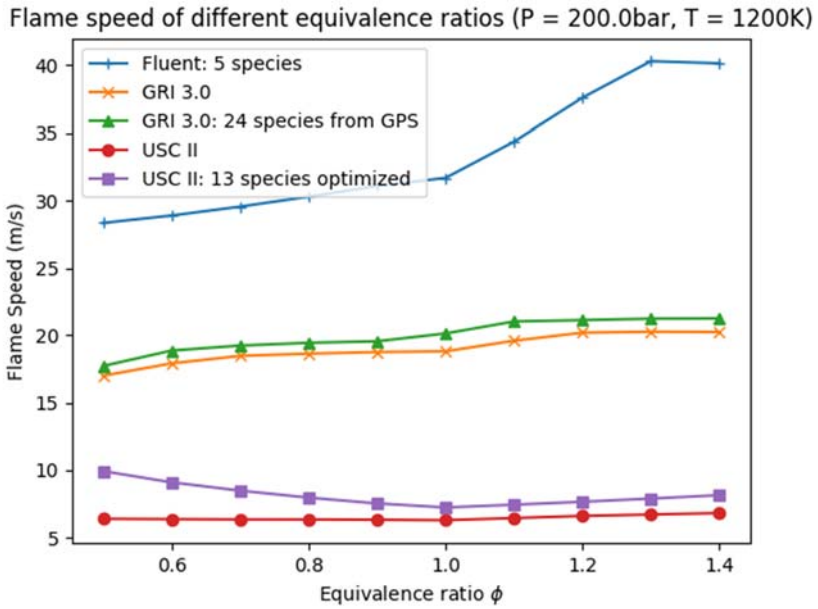

Figure 6 **Laminar flame speed (unit: m/s) of different equivalence ratios for different kinetic models with 200 bar and initial temperature 1200K**

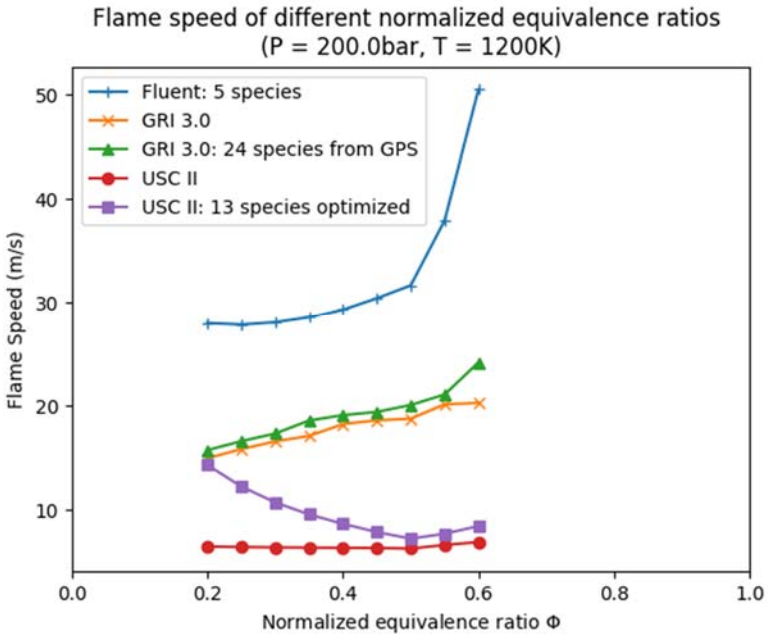

Figure 7 Laminar flame speed (unit: m/s) of different normalized equivalence ratios for different kinetic models with 200 bar and initial temperature 1200K

The comparisons of autoignition delay and laminar flame speed of the global 5 species kinetic model from Fluent, the optimized 13 species kinetic model, the 24 species simplified from GRI 3.0 by GPS [11], are shown from Figure 4 to Figure 7. The Figure 4 is the autoignition delay results at 200 bar and stoichiometric equivalence ratio and Figure 5 is the laminar flame speed results in 200 bar and 800K, while Figure 6 and Figure 7 are the laminar flame speed of 200 bar and 1200K. Notice the Figure 7 uses the normalized equivalence ratio, which is defines by $\Phi = \phi/(1+\phi)$, where φ is the equivalence ratio. All the data are calculated with Cantera [13]. Autoignition delay results in Figure 4 show that from the higher initial temperature ($T > 1000K$), the GRI 3.0 and the 24 species model simplified from it have the shorter autoignition delay than the USC Mech II and the 13 species model. Furthermore, the 5 species model from Fluent has the shortest autoignition delay, which can be explained by its over simplified mechanism. However, for the lower initial temperature ($T < 1000K$), the situations are opposite. The 5 species model, 24 species model and GRI 3.0 give the larger autoignition delay, which means they are more sensitive to the initial temperature in the supercritical CO2 condition and lack some lower temperature mechanisms. Moreover, the laminar flame speed results in Figure 6 and Figure 7 show that the USC Mech II and the 13 species model have the lower flame speed, since their autoignition delays are larger than other mechanisms. However, the results show the abnormal situations in sCO_2 condition that the 13 species model has the larger flame speed at the lean side, but the 5 species model has the faster flame speed at the rich side, due to their mechanisms.

The simulation conducted with the ANSYS Workbench [5] uses a tube with two groups of injectors designed by DesignModeler [5] and shown Figure 8. The first row of eight circumferential injectors is for O_2 and second set is for CH_4. During the combustor process, the CO_2 stream at 1200K enters the crossflow combustor from the left side, while O_2 and CH_4 are then mixed downstream. All inlets are set as mass flow rate inlets in Fluent, and with a pressure outlet boundary condition downstream, while the wall is set to adiabatic and not reactive. Other boundary conditions are shown in Figure 8.

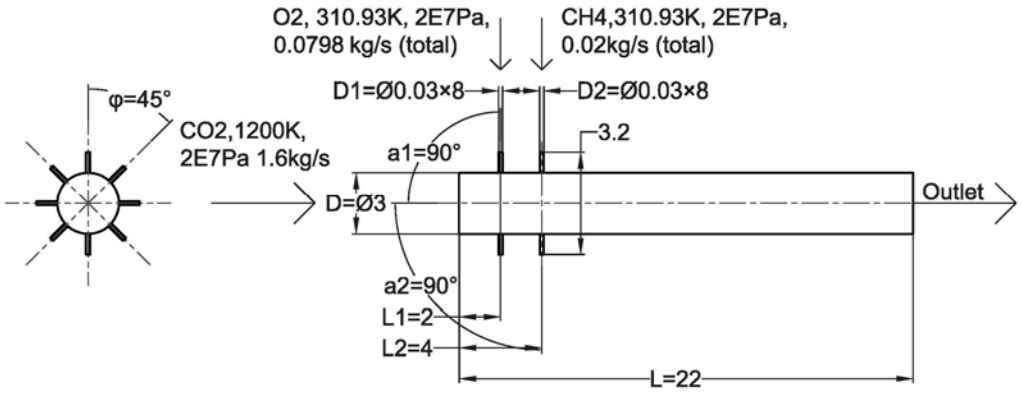

Figure 8. The geometry of crossflow combustor model (unit: inch)

An unstructured mesh was developed consisting of 783,936 elements and 193,653 nodes. A transition part was designed between the small scale injector and large scale tube, which would smooth the mesh size and increase the ability of simulations to converge. In addition, 10 inflation layers were calculated near the boundary of the main flow. The injector has a 0.1 inch length flow without the small size grids before injecting into the main flow. The k-epsilon model [14] was used for turbulent flow and the Eddy-Dissipation Concept (EDC) model [15] was used for turbulence-chemistry interaction in species transport model with Chemkin-CFD solver. The species are viewed as ideal-gas mixtures and the ideal-gas-mixing law for thermodynamic properties is used for simplicity. The SIMPLE method is used for the solution scheme, PRESTO! (PREssure STaggering Option) is used for pressure, 1st order upwind scheme was used for turbulence and 2nd order scheme was used for other variables. Mass flow rate monitors were set at the outlet. When the mass flow rate, the temperature field, the maximum temperature, and the mass of H_2O were constant, the steady state of the system was reached.

The results for a quarter sector of the model are shown from Figure 9 to Figure 15, where the lower part is symmetric mirror from the upper part in each subfigure. Notice that the scale of Figure 13 for CO mass fraction of 5 species model is different with other models. Furthermore, the normalized equivalence ratio we used in Figure 15 is also defines by $\Phi = \phi/(1+\phi)$, where φ is the equivalence ratio. Therefore the normalized equivalence ratio will vary from 0 (leanest side) to 1 (richest side), similarly to Figure 7.

The temperature contours in Figure 9 show that the 5 species model gives a faster temperature raising due to its over simplified mechanism, which can also explain its reaction zone near the injection of CH_4 and O_2 in Figure 10 and the less amount of CO in Figure 13. Then, the 13 species model has a slowest temperature raising and a lower final temperature in Figure 9, before its flowing out the tube. Since the 13 species model is simplified from USC Mech II, and both them have the larger autoignition delay as shown in Figure 4. In addition, the higher mass fraction region of the 13 species model for CH_4 and O_2 are also larger than other two models in Figure 11 and Figure 12, and the reaction zone of 13 species model is near the outlet of the tube in Figure 10. Finally, 24 species model, presents a slower temperature increasing in the Figure 9, compared with the 5 species model, but faster than the 13 species model, due the same reason of the autoignition delay in Figure 4. Besides, in Figure 13, the higher CO mass fraction near the wall can be viewed as the lack of the O_2, which is shown in Figure 12, and the boundary layer effect, due to 10 inflation layers generated near the wall.

With the results from Fluent, suggestion can be given for the kinetic models selection. When the researcher choose the mechanism, if a faster chemistry and time-saving simulation is expected, 5 species model would be a good choice and it is already built in Fluent, which can be easily converted to other formats used in Cantera[13] etc. However, if the detailed radicals are also hoped with the faster chemistry, then the 24 species kinetic model from GRI 3.0 would be suggested. However, if the slower chemistry with loner autoignition delay and slower flame speed is needed, the 13 species kinetic model simplified and optimized from USC Mech II can be a choice. Therefore, the research can select the kinetic model based on their research focus.

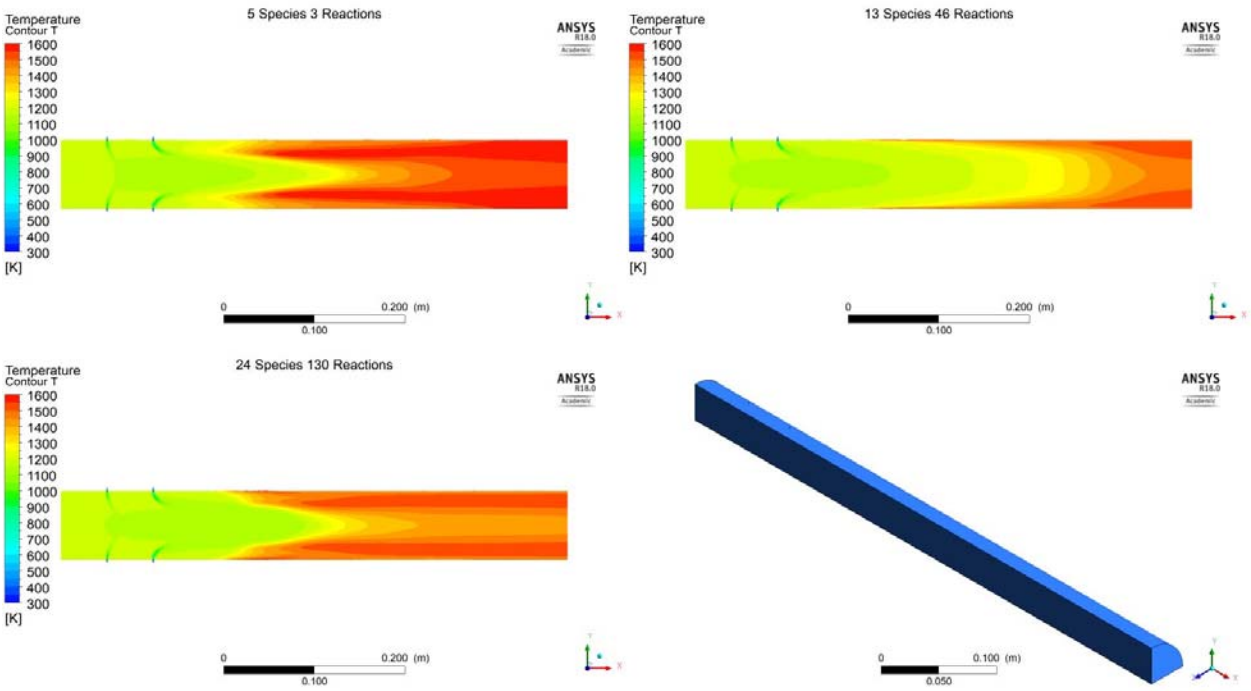

Figure 9 Temperature contours of the global 5 species kinetic model from Fluent, the optimized 13 species kinetic model from USC Mech II, and the 24 species kinetic model from GRI Mech 3.0

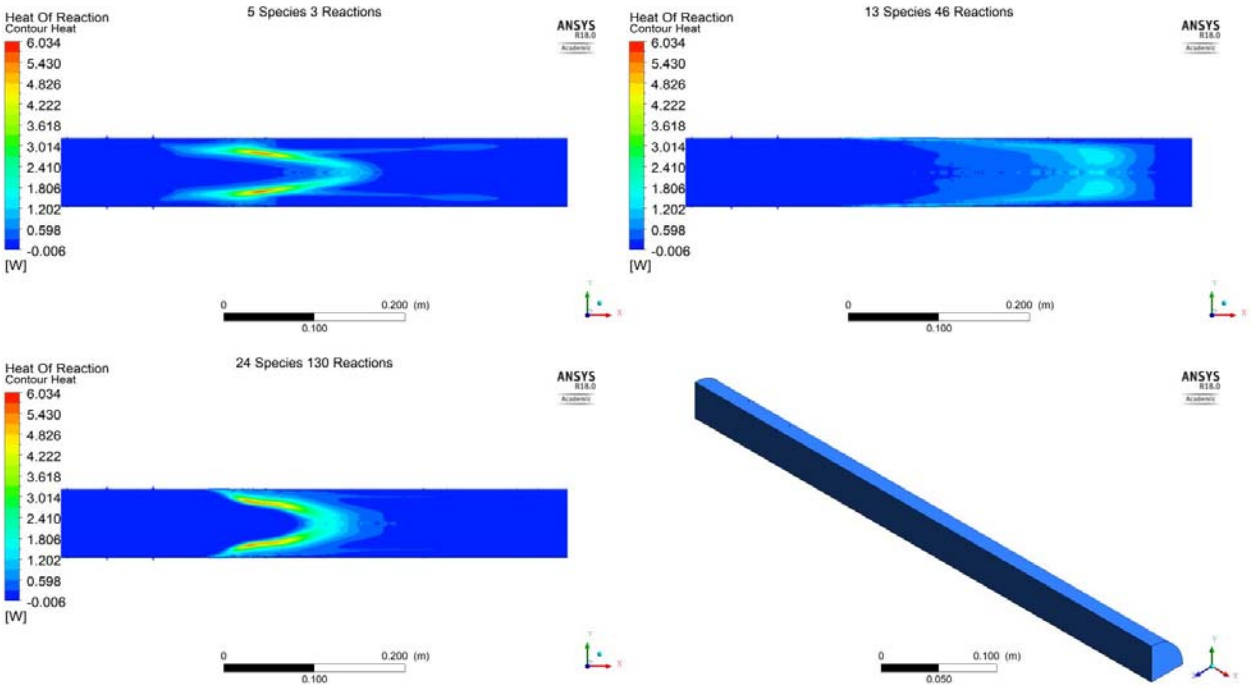

Figure 10 Heat of reactions contours of the global 5 species kinetic model from Fluent, the optimized 13 species kinetic model from USC Mech II, and the 24 species kinetic model from GRI Mech 3.0

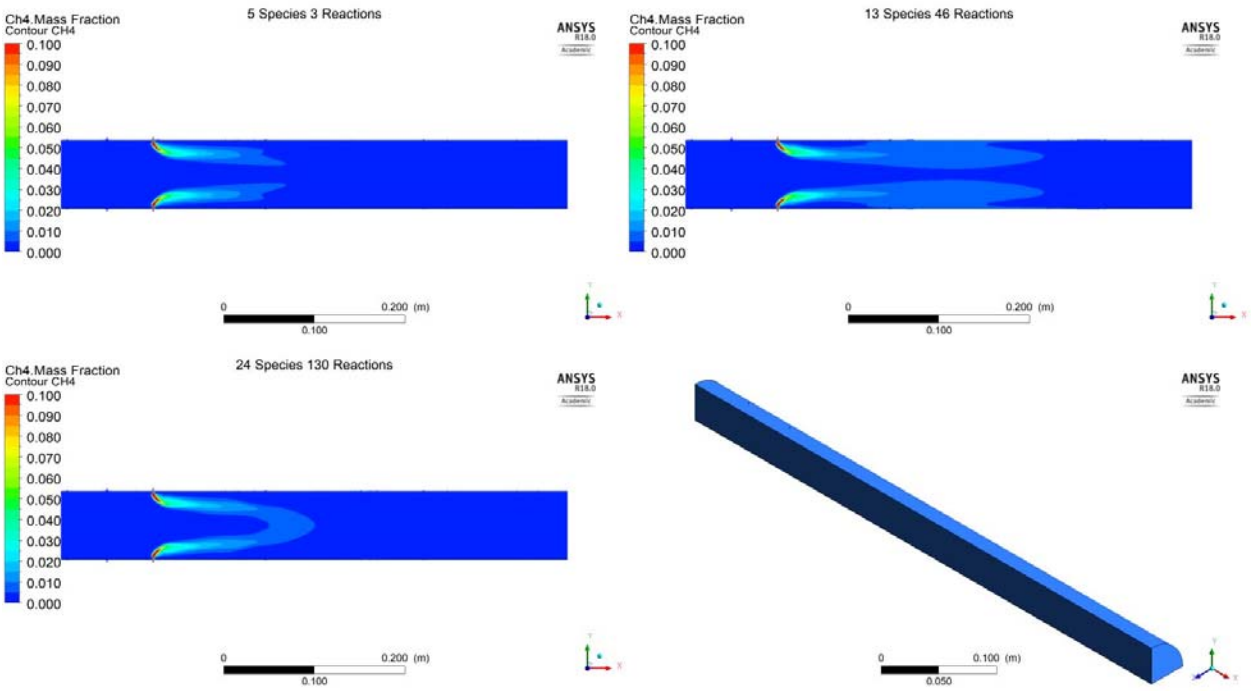

Figure 11 CH_4 mass fraction contours of the global 5 species kinetic model from Fluent, the optimized 13 species kinetic model from USC Mech II, and the 24 species kinetic model from GRI Mech 3.0

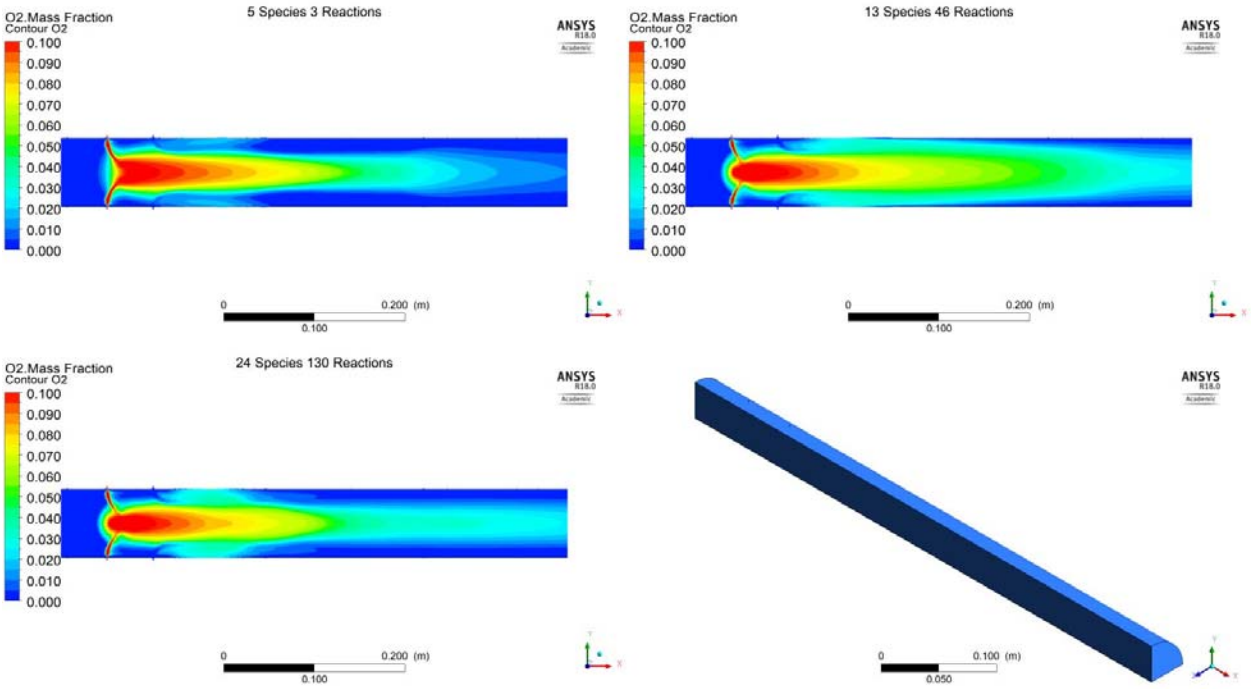

Figure 12 O_2 mass fraction contours of the global 5 species kinetic model from Fluent, the optimized 13 species kinetic model from USC Mech II, and the 24 species kinetic model from GRI Mech 3.0

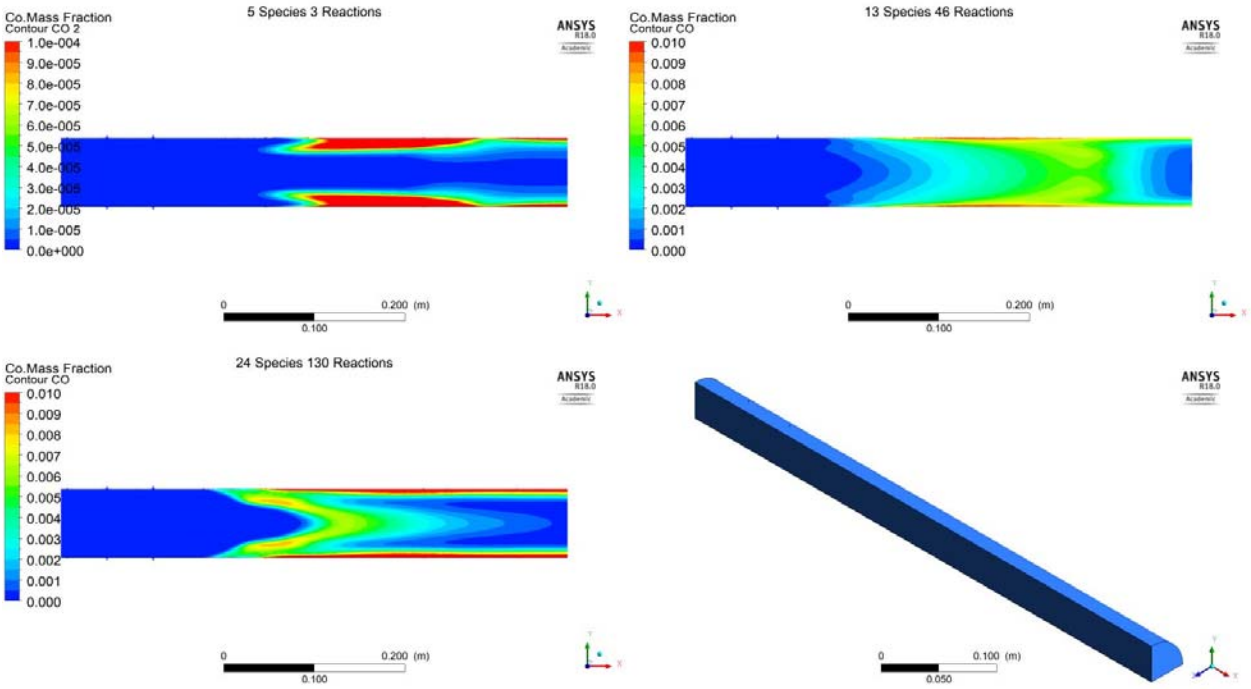

Figure 13 CO mass fraction contours of the global 5 species kinetic model from Fluent, the optimized 13 species kinetic model from USC Mech II, and the 24 species kinetic model from GRI Mech 3.0 (different scale for 5 species model)

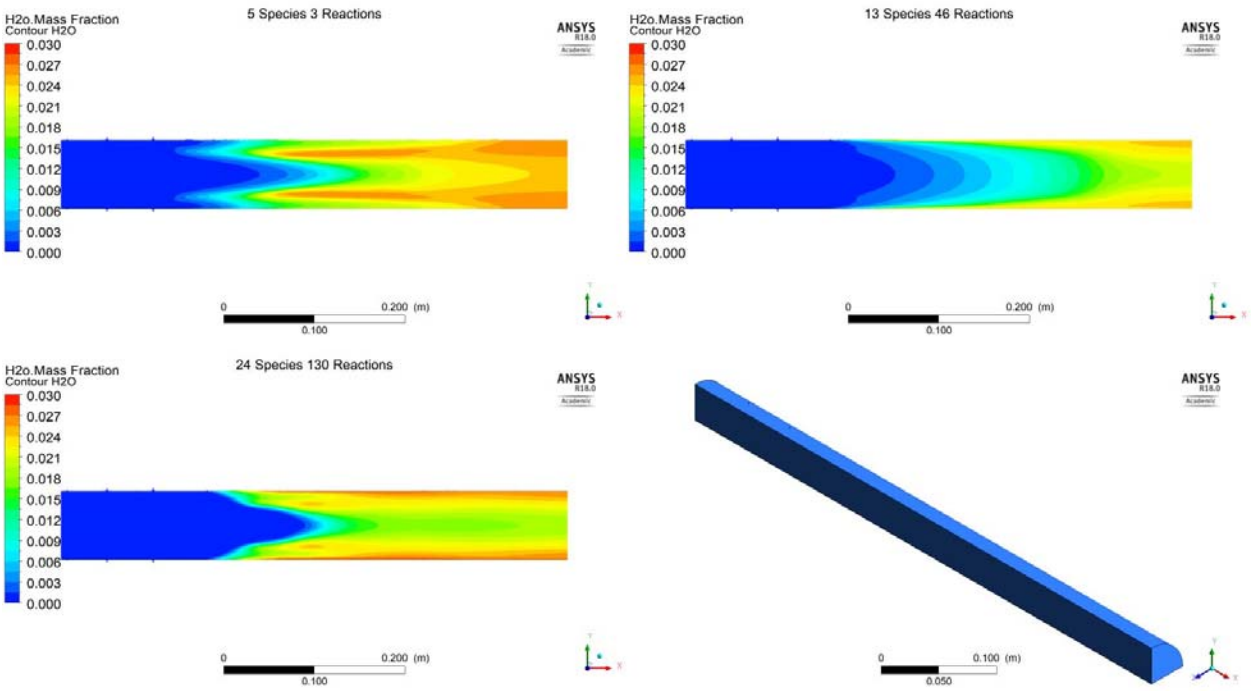

Figure 14 H_2O mass fraction contours of the global 5 species kinetic model from Fluent, the optimized 13 species kinetic model from USC Mech II, and the 24 species kinetic model from GRI

Mech 3.0

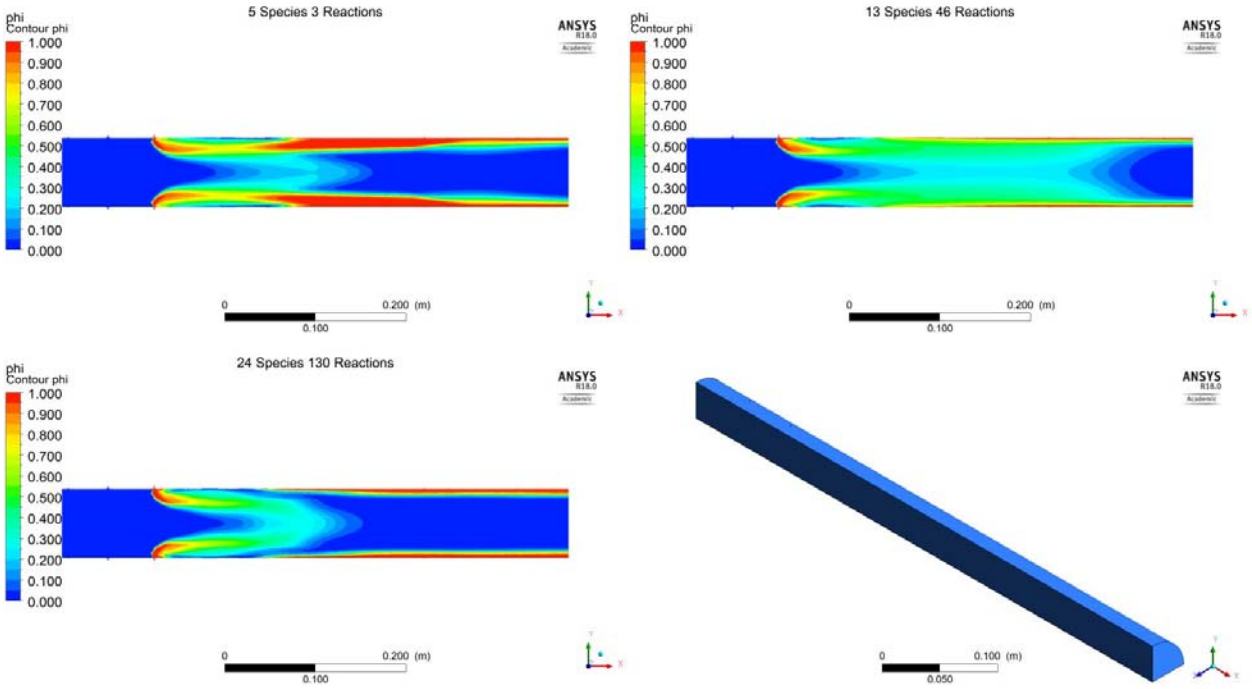

Figure 15 Normalized equivalence ratio contours of the global 5 species kinetic model from Fluent, the optimized 13 species kinetic model from USC Mech II, and the 24 species kinetic model from GRI Mech 3.0 model

SUMMARY

In the present work, different kinetic models are evaluated for the first time using autoignition delays at SCO_2 condition. USC Mech II which has the overall best agreement is selected for further reduction and numerical simulation. Then an optimized 13 species kinetic model is developed and evaluated. This kinetic model is obtained from USC Mech II using the Global Pathway Selection reduction algorithm and optimized using a genetic algorithm. The error of the optimized 13 species kinetic model is evaluated using closed zero-dimensional reactor and the maximum error is less than 12%, for the conditions of pressure ranging from 150 atm to 300 atm, temperature from 900 K to 1800 K and equivalence ratio from 0.7 to 1.3. This 13 species kinetic model is then applied in the simulation of a generic jet in crossflow reactor. The numerical simulation employing the 13 species model, a global 5 species model and a 24 species model from GRI 3.0 were compared. The results showed that the simulation is sensitive to kinetic models, and the simulation using 13 species kinetic model shows longer autoignition delay, therefore the reaction zone is located further downstream. Also, researcher should select the kinetic model based on their research focus.

REFERENCES

[1] Coogan, S., Gao, X., McClung, A., and Sun, W., "Evaluation of Kinetic Mechanisms for Direct Fired Supercritical Oxy-Combustion of Natural Gas," ASME Turbo Expo 2016: Turbomachinery Technical Conference and Exposition, 2016, pp. GT2016-56658.

[2] Y. Iwai, M. Itoh, Y. Morisawa, S. Suzuki, D. Cusano and M. Harris, "Development Approach to the Combustor of Gas Turbine for Oxy-fuel, Supercritical CO_2 Cycle," in Proceedings of ASME Turbo Expo 2015: Turbine Technical Conference and Exposition, Montreal, Canada, June 15-19, 2015, pp. GT2015-43160.

[3] D. Healy, H. Curran, S. Dooley, J. Simmie, D. Kalitan, E. Petersen, G. Bourque, Methane/propane mixture oxidation at high pressures and at high, intermediate and low temperatures, Combust. Flame 155 (3) (2008) 451–461, doi:10. 1016/j.combustflame.2008.06.008.
[4] Hai Wang, Xiaoqing You, Ameya V. Joshi, Scott G. Davis, Alexander Laskin, Fokion Egolfopoulos & Chung K. Law, USC Mech Version II. High-Temperature Combustion Reaction Model of H2/CO/C1-C4 Compounds. http://ignis.usc.edu/USC_Mech_II.htm, May 2007.
[5] ANSYS® Academic, Release 17.1, ANSYS, Inc.
[6] Gregory P. Smith, David M. Golden, Michael Frenklach, Nigel W. Moriarty, Boris Eiteneer, Mikhail Goldenberg, C. Thomas Bowman, Ronald K. Hanson, Soonho Song, William C. Gardiner, Jr., Vitali V. Lissianski, and Zhiwei Qin http://www.me.berkeley.edu/gri_mech/.
[7] “Chemical-Kinetic Mechanisms for Combustion Applications,” Mechanical and Aerospace Engineering (Combustion Research), University of California at San Diego, 04-Oct-2014.
[8] X. Shen, X. Yang, J. Santner, J. Sun, Y. Ju, Experimental and kinetic studies of acetylene flames at elevated pressures. Proceedings of the Combustion Institute, 35 (2015) 721-728.
[9] H. Zhao, J. Fu, F.M. Haas, Y. Ju, Effect of prompt dissociation of formyl radical on 1,3,5-trioxane and CH_2O laminar flame speeds with CO_2 dilution at elevated pressure, Combustion and Flame, 183 (2017) 253–260.
[10] Y. Li, C-W. Zhou, K.P. Somers, K. Zhang, H.J. Curran The Oxidation of 2-Butene: A High Pressure Ignition Delay, Kinetic Modeling Study and Reactivity Comparison with Isobutene and 1-Butene Proceedings of the Combustion Institute (2017) 36(1) 403–411.
[11] Gao, X., Yang, S., and Sun, W., "A global pathway selection algorithm for the reduction of detailed chemical kinetic mechanisms," Combustion and Flame, Vol. 167, 2016, pp. 238-247. doi: 10.1016/j.combustflame.2016.02.007.
[12] Mitchell, Melanie (1996). An Introduction to Genetic Algorithms. Cambridge, MA: MIT Press. ISBN 9780585030944.
[13] David G. Goodwin, Harry K. Moffat, and Raymond L. Speth. Cantera: An object- oriented software toolkit for chemical kinetics, thermodynamics, and transport processes. http://www.cantera.org, 2017. Version 2.3.0. doi:10.5281/zenodo.170284.
[14] T.-H. Shih, W. W. Liou, A. Shabbir, Z. Yang, and J. Zhu. "A New - Eddy-Viscosity Model for High Reynolds Number Turbulent Flows - Model Development and Validation". Computers Fluids. 24(3). 227–238. 1995.
[15] B. F. Magnussen. "On the Structure of Turbulence and a Generalized Eddy Dissipation Concept for Chemical Reaction in Turbulent Flow". Nineteenth AIAA Meeting, St. Louis 1981.

ACKNOWLEDGEMENTS

This work is U.S. Department of Energy (Award Number: DE-FE0025174, Program Office: Seth Lawson).